AD-A225 336

REPORT DOCUMENTATION PAGE

Form Approved
OMB No. 0704-0188

1. AGENCY USE ONLY (Leave blank)	2. REPORT DATE	3. REPORT TYPE AND DATES COVERED
	9 August 1990	Reprint

4. TITLE AND SUBTITLE
A Case Study Using Kinematic Quantities Derived From a Triangle of VHF Doppler Wind Profilers

5. FUNDING NUMBERS
PE 61101F
PR ILIR TA 5J WU AA
Contract F19628-85-K-0011
PE 61102F
PR 2310 TA G8 WU BE
Contract F19628-86-C-0092

6. AUTHOR(S)
Catherine A. Carlson*
Gregory S. Forbes

7. PERFORMING ORGANIZATION NAME(S) AND ADDRESS(ES)
Pennsylvania State University
Department of Meteorology
University Park, PA 16802

8. PERFORMING ORGANIZATION REPORT NUMBER

9. SPONSORING/MONITORING AGENCY NAME(S) AND ADDRESS(ES)
Geophysics Laboratory
Hanscom AFB, MA 01731-5000

Contract Manager: Arthur Jackson/LYP

10. SPONSORING/MONITORING AGENCY REPORT NUMBER
GL-TR-90-0193

11. SUPPLEMENTARY NOTES * NASA/Marshall Space Flight Center, Huntsville, AL
Reprinted from J of Atmospheric & Oceanic Technology, Vol 6, #5, Oct 1989

12a. DISTRIBUTION/AVAILABILITY STATEMENT
Approved for public release; distribution unlimited

12b. DISTRIBUTION CODE

13. ABSTRACT (Maximum 200 words)

Horizontal divergence, relative vorticity, kinematic vertical velocity, and geostrophic and ageostrophic winds are computed from Colorado profiler network data to investigate an upslope snowstorm in northeastern Colorado. Horizontal divergence and relative vorticity are computed using the Gauss and Stokes theorems, respectively. Kinematic vertical velocities are obtained from the surface to 9 km by vertically integrating the continuity equation. The geostrophic and ageostrophic winds are computed by applying a finite differencing technique to evaluate the derivatives in the horizontal equations of motion. Comparison of the synoptic-scale data with the profiler network data reveals that the two datasets are generally consistent. Also, the profiler-derived quantities exhibit coherent vertical and temporal patterns consistent with conceptual and theoretical flow fields of various meteorological phenomena. It is suggested that the profiler-derived quantities are of potential use to weather forecasters in that they enable the dynamic and kinematic interpretation of weather system structure to be made and thus have nowcasting and short-term forecasting value.

14. SUBJECT TERMS
Kinematic Quantities
VHF
Doppler Wind Profilers

15. NUMBER OF PAGES
10

16. PRICE CODE

17. SECURITY CLASSIFICATION OF REPORT	18. SECURITY CLASSIFICATION OF THIS PAGE	19. SECURITY CLASSIFICATION OF ABSTRACT	20. LIMITATION OF ABSTRACT
Unclassified	Unclassified	Unclassified	SAR

Reprinted from JOURNAL OF ATMOSPHERIC AND OCEANIC TECHNOLOGY, Vol. 6, No. 5, October 1989
American Meteorological Society

A Case Study Using Kinematic Quantities Derived from a Triangle of VHF Doppler Wind Profilers

CATHERINE A. CARLSON

NASA/Marshall Space Flight Center, Huntsville, Alabama

GREGORY S. FORBES

Department of Meteorology, Pennsylvania State University, University Park, Pennsylvania

(Manuscript received 30 May 1988, in final form 22 March 1989)

ABSTRACT

Horizontal divergence, relative vorticity, kinematic vertical velocity, and geostrophic and ageostrophic winds are computed from Colorado profiler network data to investigate an upslope snowstorm in northeastern Colorado. Horizontal divergence and relative vorticity are computed using the Gauss and Stokes theorems, respectively. Kinematic vertical velocities are obtained from the surface to 9 km by vertically integrating the continuity equation. The geostrophic and ageostrophic winds are computed by applying a finite differencing technique to evaluate the derivatives in the horizontal equations of motion. Comparison of the synoptic-scale data with the profiler network data reveals that the two datasets are generally consistent. Also, the profiler-derived quantities exhibit coherent vertical and temporal patterns consistent with conceptual and theoretical flow fields of various meteorological phenomena. It is suggested that the profiler-derived quantities are of potential use to weather forecasters in that they enable the dynamic and kinematic interpretation of weather system structure to be made and thus have nowcasting and short-term forecasting value.

1. Introduction

The Colorado profiler network has provided meteorologists with an opportunity to continuously observe the upper-level winds with high temporal and spatial resolution. Computations of profiler network-derived quantities such as horizontal divergence, relative vorticity, kinematic vertical velocity, and ageostrophic and geostrophic winds reveal mesoscale and synoptic-scale motions associated with short waves, jet streaks, and upper-level fronts. Zamora et al. (1987) and Augustine and Zipser (1987) have shown that the information derived from the Colorado profiler network can be used to diagnose thunderstorm activity in the Central Plains states. A case study is presented below to illustrate the usefulness of the profiler network-derived kinematic quantities in understanding the nature of a so-called "upslope" snowstorm in northeastern Colorado.

The Doppler wind profiler derives its signal from the backscatter of the transmitted signal by inhomogeneities in the radio refractive index. These inhomogeneities are the result of turbulent variations in temperature and humidity. Gage and Balsley (1978), Balsley (1981), and Balsley and Gage (1982) give a detailed review of the Doppler wind profiler measurement technique.

Strauch et al. (1984) describe the design, data processing and performance characteristics of the Colorado profiler network. The three Doppler wind profilers used in this investigation were sited near Fleming, Flagler, and Platteville, Colorado. The distance between each of these profilers is approximately 170 km, which is less than half the distance between rawinsonde sites in the National Weather Service network. Hourly averaged high resolution data ranging from 3 to 9 km MSL at intervals of 300 m were used to calculate the kinematic quantities.

2. Computation of kinematic quantities from a triangle of Doppler wind profilers

Horizontal divergence and relative vorticity are computed using a line integral method that implements Gauss' theorem,

$$\text{div} \cdot A = \oint_s \mathbf{V} \cdot \mathbf{n} ds = \int_A \nabla \cdot \mathbf{V} dA, \qquad (1)$$

and Stokes' theorem,

$$\text{vor} \cdot A = \oint_s \mathbf{V} \cdot ds = \int_A (\nabla \times \mathbf{V}) \cdot \mathbf{n} dA, \qquad (2)$$

Corresponding author address: Catherine A. Carlson, Space Science Lab/ES44, NASA/Marshall Space Flight Center, Marshall Space Flight Center, AL 35812.

respectively. The unit vector **n** is directed normal to the surface and outward, the unit vector **s** is directed along the surface in a counterclockwise direction, and ds is a unit length along the surface. In applying these formulae to profiler triangle data, the integrals are expressed as summations along the three sides. The wind is assumed to vary linearly between the profiler sites, and the quantities derived from the above equations represent areal averaged values applicable to the centroid of the triangle.

Vertical velocities are obtained from a triangle of profilers through implementation of the kinematic method, which vertically integrates the continuity equation

$$\frac{\partial(\rho w)}{\partial z} = -\rho \nabla_H \cdot \mathbf{V}_H, \tag{3}$$

where ∇_H is the two-dimensional divergence operator and $\mathbf{V}_H$ is the two-dimensional horizontal velocity. The vertical velocity is then computed level by level by summing the right-hand side,

$$W_N = \frac{W_0 \rho_0}{\rho_N} + \sum_{n=1}^{N} \frac{(\rho_{N-1}\,\mathrm{div}_{N-1} + \rho_N\,\mathrm{div}_N)}{2(\rho_N + \rho_{N-1})} \Delta Z_N. \tag{4}$$

Here W_N is the vertical velocity at level N, ρ_{N-1} and ρ_N are the air density at levels $N-1$ and N, and ρ_0 is the air density computed at the surface. The lower boundary condition, W_0, is obtained by computing surface orographic effects. The continuity equation is integrated in two steps. The first step integrates divergence from the surface to 3 km using values calculated from the surface observation network and the lowest profiler measurement level. In this step, vertical motions are assumed to vary linearly from the surface to 3 km. The second step integrates divergence from 3 to 9 km in twenty-one 300 m increments, using the 22 values of individual level divergences computed from (1). Densities were obtained from NWS rawinsondes released at Denver.

Because the kinematic method is sensitive to an accumulation of error at the termination of integration, a correction scheme is implemented which adjusts the divergence values at each profiler level by a constant. The constant is computed using the equation

$$K = \frac{-W(z_{STR})}{z_{STR} - z_0}, \tag{5}$$

which forces the vertical motions at 14 km to equal zero. Here $W(z_{STR})$ is the kinematic vertical velocity at 14 km, and is obtained from low resolution profiler data which ranges from 4 to 14 km above mean sea level at 900 m increments. The value of z_{STR} is 14 km, while z_0, the lowest altitude whose divergence is computed from the low resolution data, is 4 km. The constant was then applied to the high resolution data. The constant varied with time, but was on the order of $\pm 1 \times 10^{-5}\ \mathrm{s}^{-1}$.

The ageostrophic winds are determined using the following equations, in which viscous and turbulent processes are neglected:

$$\bar{u}_{ag} = -\frac{1}{f}\left[\frac{\partial \bar{v}}{\partial t} + \bar{u}\frac{\partial v}{\partial x} + \bar{v}\frac{\partial v}{\partial y} + \bar{w}\frac{\partial \bar{v}}{\partial z}\right] \tag{6}$$

$$\bar{v}_{ag} = \frac{1}{f}\left[\frac{\partial \bar{u}}{\partial t} + \bar{u}\frac{\partial u}{\partial x} + \bar{v}\frac{\partial u}{\partial y} + \bar{w}\frac{\partial \bar{u}}{\partial z}\right]. \tag{7}$$

In this context the overbar denotes the areal averaged value or centroid value of the velocity component (rather than a single station temporal average). To compute $\bar{u}$ and $\bar{v}$, an average value of u and v is computed for each side of the triangle using the winds from the two profilers which define that side of the triangle. The side-averaged value is then weighted by the distance between the two profilers. The three weighted values are then added and divided by the perimeter of the profiler triangle.

The spatial derivatives are calculated by a finite difference scheme after the u and v components of the three profiler sites are linearly interpolated to an unevenly spaced grid. The method of linear interpolation is described below. The latitude and longitude of the profiler sites are converted to an orthogonal Cartesian coordinate system. The origin of the coordinate system is located at the southwest corner of the triangle with the western site intersecting the y axis and the southern site intersecting the x axis as shown in Fig. 1. The equations used for the conversions are

$$x_N = 111.0[(\mathrm{LON}_N - \mathrm{LONMIN})(\cos(\mathrm{LATCEN}))] \tag{8}$$

$$y_N = 111.0(\mathrm{LAT}_N - \mathrm{LATMIN}). \tag{9}$$

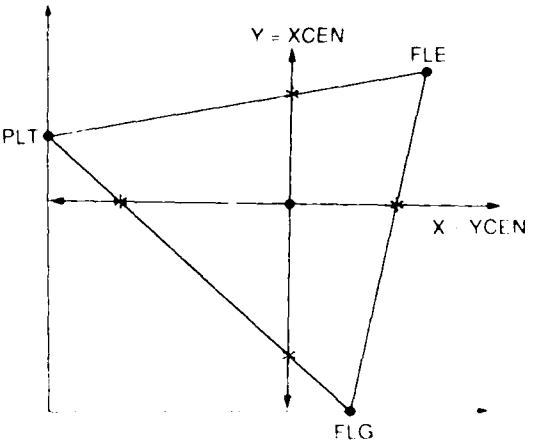

FIG. 1. Schematic of the interpolation scheme used to fit the irregularly spaced profiler winds to a grid. The four asterisks denote the four grid points used by the finite differencing scheme.

where LATMIN and LONMIN are the minimum latitude and longitude of the three profiler sites, LAT_N and LON_N are the latitude and longitude of the individual profiler sites, and LATCEN is the average latitude of the three profiler sites. The equations for computing the x and y coordinates (XCEN and YCEN) of the centroid of the triangle are

$$\text{XCEN} = \frac{x_1 + x_2 + x_3}{3} \tag{10}$$

$$\text{YCEN} = \frac{y_1 + y_2 + y_3}{3}. \tag{11}$$

Then x and y axes are drawn through the centroid of the triangle to intersect the sides of the triangle. The x and y coordinates are computed at the four points of intersection, and the u and v components are interpolated to each of the four points. The derivatives are computed using the equations

$$\frac{\partial u}{\partial x} = \frac{u(\text{XMAX, YCEN}) - u(\text{XMIN, YCEN})}{\text{XMAX} - \text{XMIN}} \tag{12}$$

$$\frac{\partial v}{\partial x} = \frac{v(\text{XMAX, YCEN}) - v(\text{XMIN, YCEN})}{\text{XMAX} - \text{XMIN}} \tag{13}$$

$$\frac{\partial u}{\partial y} = \frac{u(\text{XCEN, YMAX}) - u(\text{XCEN, YMIN})}{\text{YMAX} - \text{YMIN}} \tag{14}$$

$$\frac{\partial v}{\partial y} = \frac{v(\text{XCEN, YMAX}) - v(\text{XCEN, YMIN})}{\text{YMAX} - \text{YMIN}}. \tag{15}$$

It should be noted that the ageostrophic and geostrophic winds computed by the above method contain errors in the estimation of the spatial derivatives due to the remapping of the u and v components to a grid. Doswell and Caracena (1988) have shown that these errors can be eliminated by computing the derivatives with a linear vector point function or a line integral method.

The derivatives of $\partial\bar{u}/\partial t$ and $\partial\bar{v}/\partial t$ are computed as centered-in-time finite differences of $\bar{u}$ and $\bar{v}$. The geostrophic components are derived by subtracting the ageostrophic components from $\bar{u}$ and $\bar{v}$. The ageostrophic and geostrophic winds are areal averaged values pertaining to the centroid of the triangle.

3. Case study from 1200 UTC 28 September to 2300 UTC 29 September 1985

A Colorado upslope snowstorm during the period from 1200 UTC 28 September to 2300 UTC 29 September 1985 was investigated by combining conventional radar, surface, and rawinsonde observations with the observed winds and derived quantities of the Doppler wind profiler network. Though the low-level flow was generally upslope, the kinematic quantities derived from the profiler data suggest that important weather systems traveling aloft exerted greater control over the precipitation intensity. In the sections that follow, the synoptic-scale features are introduced briefly using conventional data. Details of the weather are then examined using profiler data.

a. Synoptic environment

Prior to 1200 UTC 28 September 1985, a high pressure system with 1034 mb center moved eastward through southern Canada channeling cold air along the east slopes of the Rocky Mountains. A shallow cold dome developed over the region as the easterly flow from the anticyclone dammed the cold air along the mountain slopes. This cold pocket of air remained over the profiler network [but beneath 3 km mean sea level (MSL), the lowest level sampled by the profiler] throughout the case, and served as an overrunning surface for the moist southwesterly flow aloft.

According to the rawinsonde network data, a 700 mb short-wave trough with an associated cold front passed through the profiler network between 1200 UTC 28 to 0000 UTC 29 September. During this period, the atmosphere became saturated from 700 to 500 mb as the southwesterly flow associated with an approaching 500 mb trough advected moisture from the southwest region. Following the passage of the 500 mb front between 0000 UTC and 1200 UTC 29 September, the atmosphere underwent strong cold and dry advection. The 300 mb synoptic charts at 1200 UTC 28 and 0000 UTC 29 September, shown in Fig. 2, indicate that the axis of a southwesterly jet stream with an embedded jet streak was initially north of the profiler network and drifted over the network by 1200 UTC 29 September. The 500 and 300 mb trough axes passed through the profiler network after 1200 UTC 29 September. The profiler winds and derived quantities are examined in the following sections for details of the structure of these synoptic-scale features.

b. Observed profiler winds

A wind shift associated with the passage of the 700 mb trough is apparent in the time–height section of the Platteville (in Fig. 3), Fleming and Flagler profiler winds at approximately 1900 UTC 28, 2200 UTC and 0800 UTC 29 September, respectively. The approach of the axis of the jet stream could also be seen over Platteville, Fleming and Flagler profiler sites beginning about 1800 UTC, 1900 UTC and 2000 UTC 28, respectively, as indicated by winds increasing to more than 30 m s^{-1}. The winds shifted from southwest to northwest as the 500 mb and 300 mb troughs passed through Platteville at 1900 UTC and 2100 UTC 29, Flagler at 2100 UTC and 2300 UTC 29. The winds at Fleming were in the process of veering to the northwest at 0000 UTC 30.

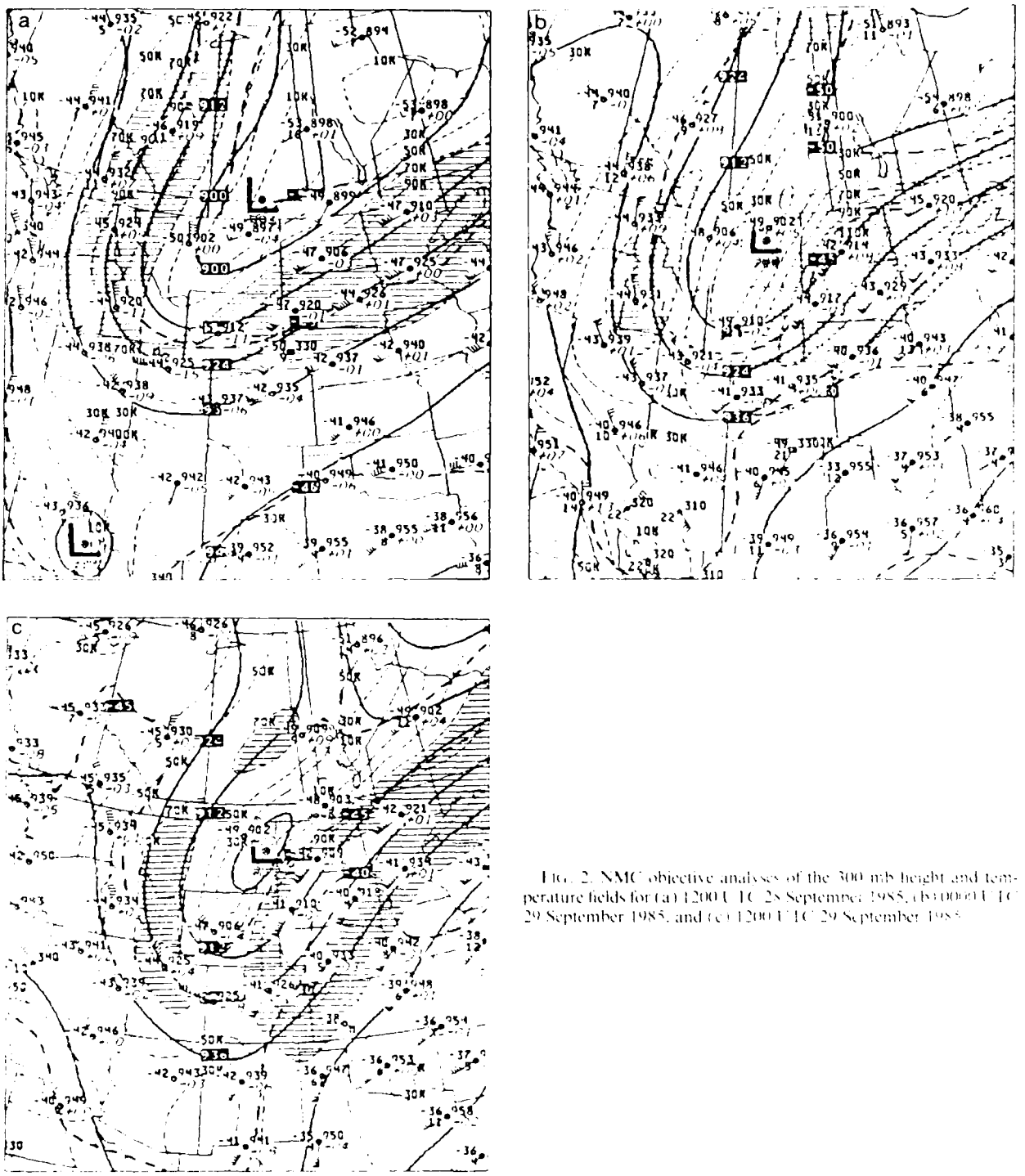

FIG. 2. NMC objective analyses of the 300 mb height and temperature fields for (a) 1200 UTC 28 September 1985, (b) 0000 UTC 29 September 1985, and (c) 1200 UTC 29 September 1985.

c. *Profiler-derived quantities*

The profiler-derived geostrophic winds, shown in Fig. 4, were much like the areal averaged winds below 5 km. As the southwesterly jet stream entered the profiler triangle, however, the middle and upper tropospheric winds were slightly greater in magnitude and more westerly in direction than the areal averaged winds, most notably near 6 to 7 km, indicating the presence of ageostrophic motions. After 1500 UTC 29 September, the geostrophic winds were also much stronger than the areal averaged winds above 7 km as the upper level trough approached the profiler site.

The profiler-derived ageostrophic winds are shown

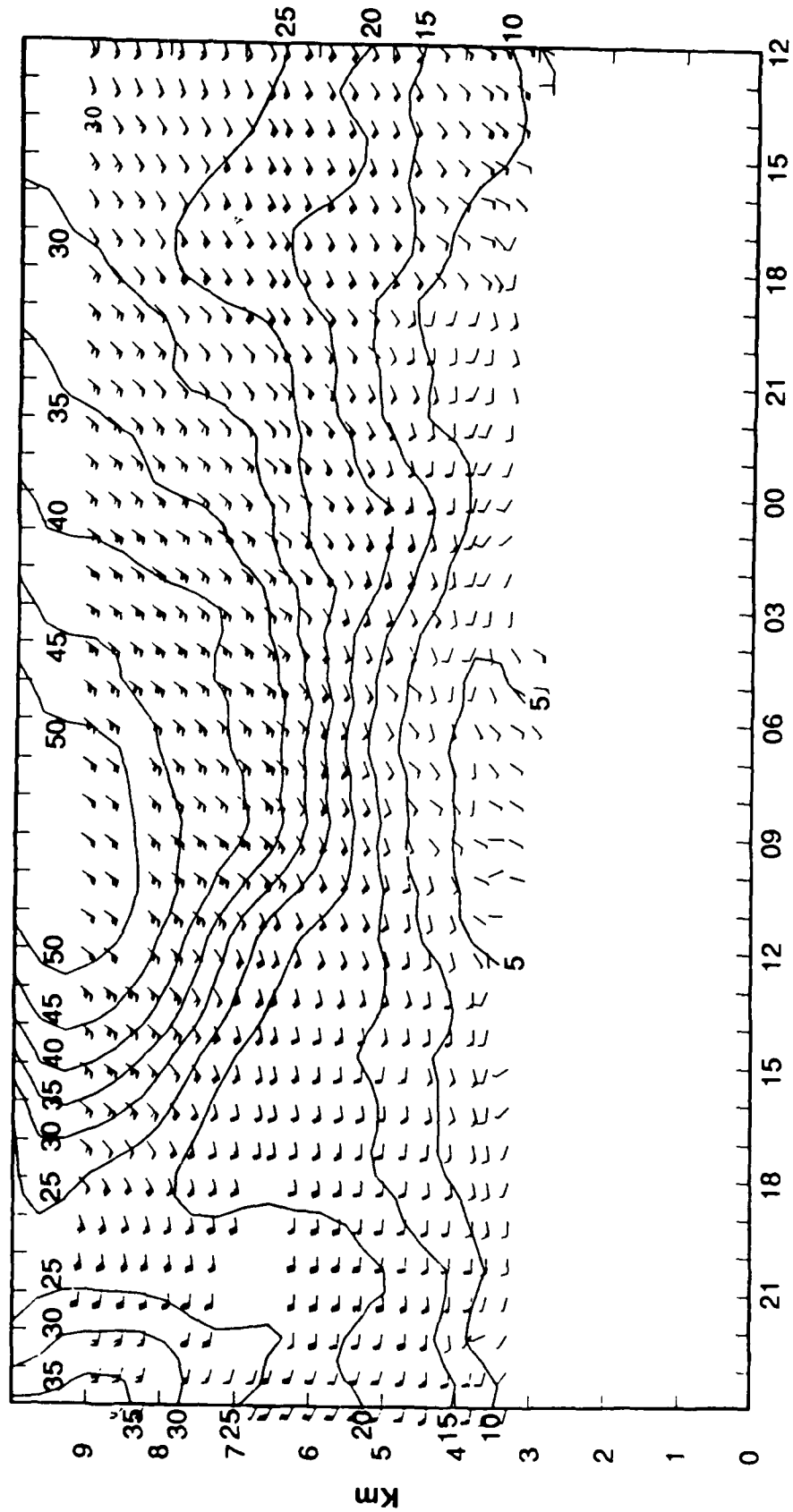

FIG. 3. Time–height section of observed winds from the Platteville profiler during the period from 1200 UTC 28 to 2300 UTC 29 September 1985. One flag represents 5.0 m s^{-1}. One pennant represents 26.0 m s^{-1}. A wind from the south points toward the top of the page. Contour interval is 5 m s^{-1}. Blank areas denote missing data points.

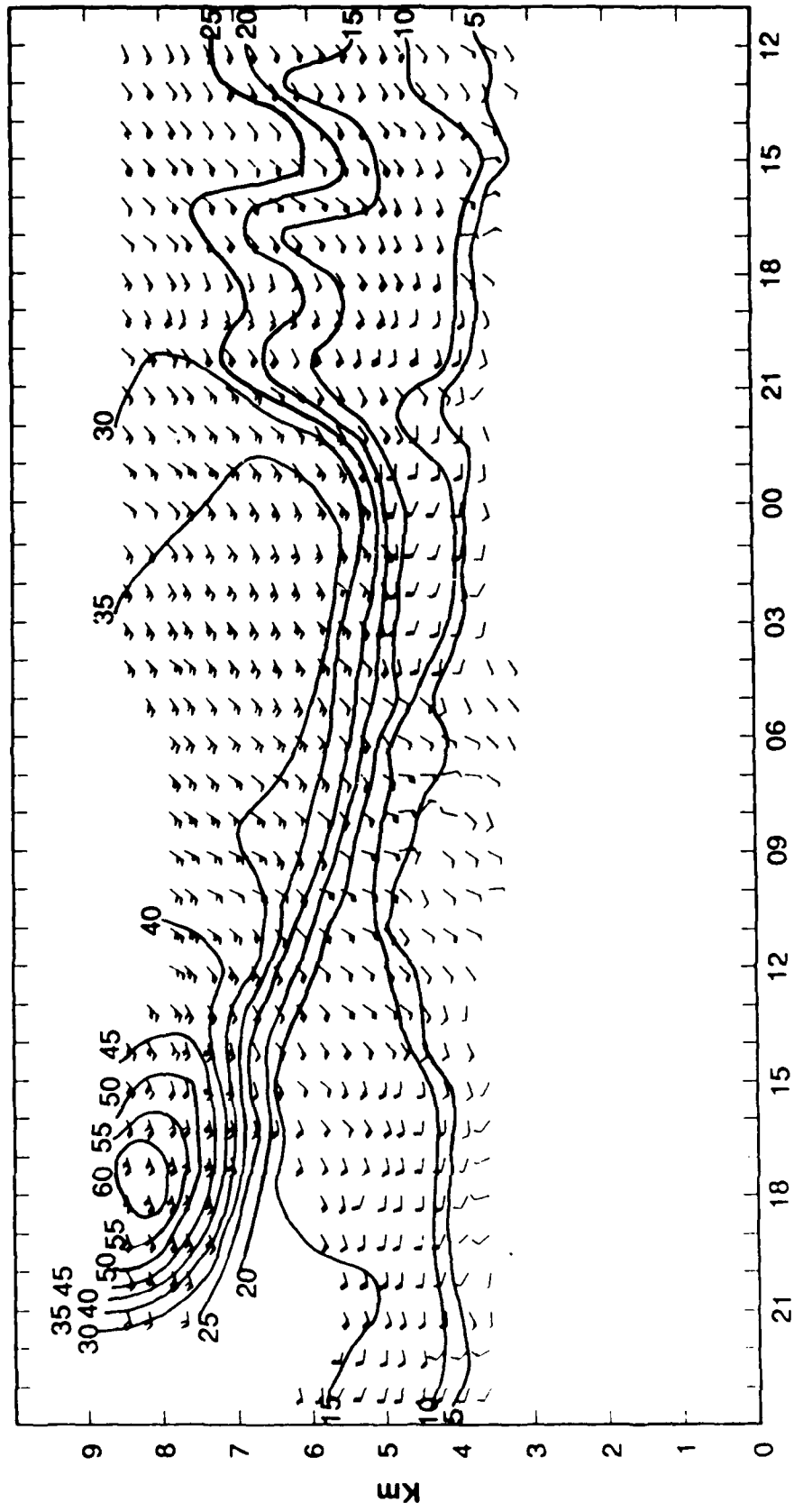

FIG. 4. Time–height section of the profiler-derived geostrophic winds during the period from 1200 UTC 28 to 2300 UTC 29 September 1985. Convention as in Fig. 3.

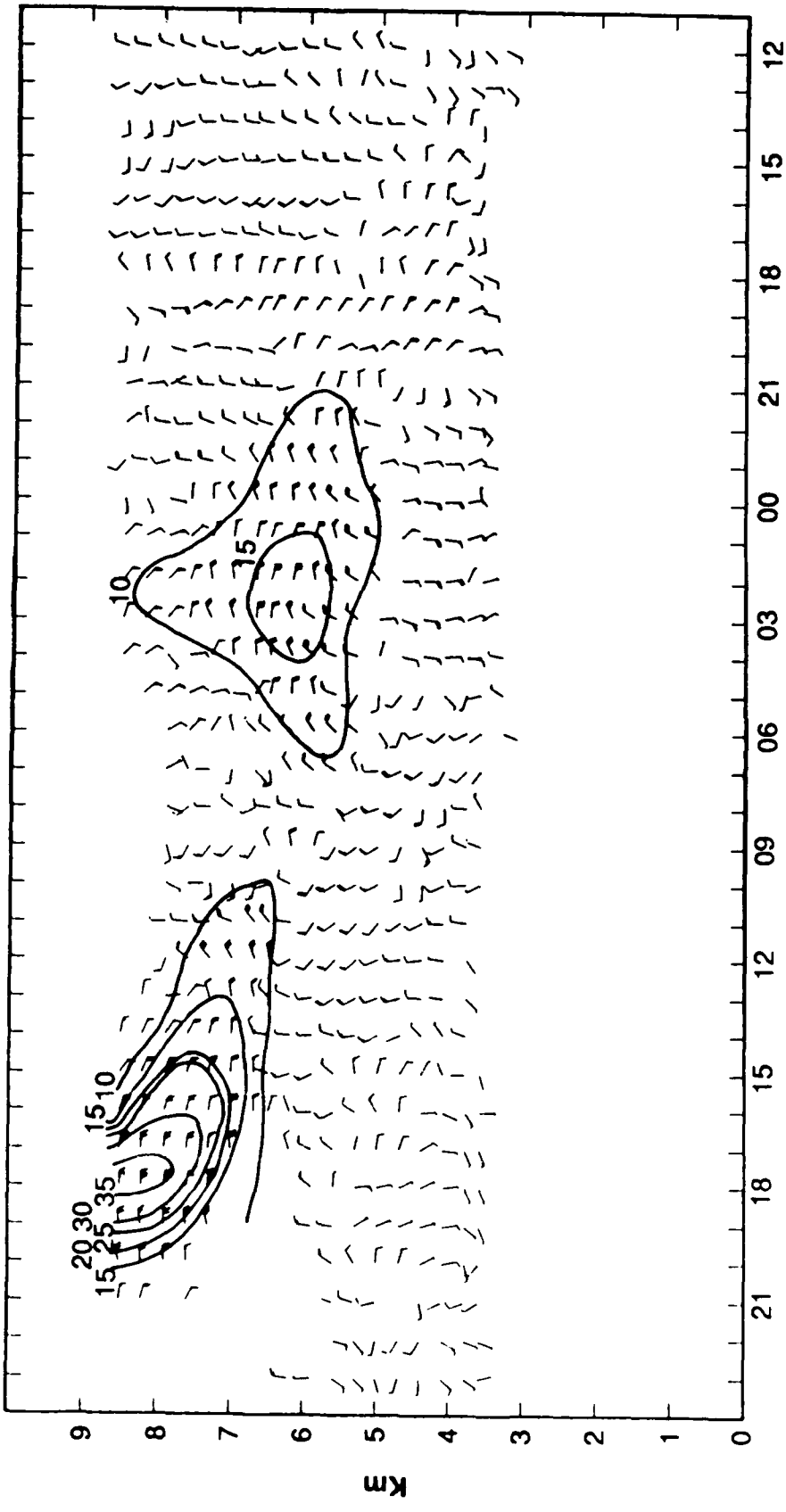

FIG. 5. As in Fig. 4 except for ageostrophic winds.

in Fig. 5. While the pattern is noisy in places, several periods of very consistent winds are evident. One feature is a sloping belt of ageostrophic east-southeasterlies that begins near 4 km MSL at 1400 UTC 28 September and continues in time to about 6 km at 0500 UTC 29 September. This is an overrunning flow rising along the frontal surface discussed earlier. This feature is primarily responsible for the precipitation event.

Above 5 km, another period of consistent ageostrophic winds occurs between 1200 UTC and 1700 UTC 28 September. Ageostrophic winds are from the north and west, which means they are directed toward the right of the observed winds. A few hours of light and/or variable ageostrophic winds follow at these levels, and then a period of consistent east-southeasterlies occurs between 0000 UTC and 0700 UTC 29 September. These ageostrophic winds are directed to the left of the jet stream. Together, this couplet suggests the passage of a jet streak over the profiler network. The profilers were in the right exit region of the streak from 1200 UTC to 1700 UTC 28 September, then near and probably south of the core of the jet streak until 0000 UTC 29 September, and in the entrance region of the streak until 0700 UTC 29 September. Profiler-measured wind speeds peaked over the profiler network around 1200 UTC 29 September as the axis of the jet stream passed over the network.

After 1100 UTC 29 September, the ageostrophic winds above 6.5 km were from the east. This is the period when the 300 mb trough axis passed through the network. Observed winds were westerly at this time, and the easterly ageostrophic winds are interpreted as being a response to the large cyclonic curvature. Specifically, in a cyclonically curved flow, balanced winds will be slower than geostrophic.

The profiler-derived horizontal divergence values, shown in Fig. 6, indicated a convergence zone sloping with height to about 6 km beginning at 1600 UTC 28 September. This convergence zone was related to the synoptic-scale cold front which passed through the profiler triangle. During this period from 2300 UTC 28 to 0300 UTC 29 September, convergence in the lower atmosphere and divergence in the upper atmosphere was maximized. This period coincided with the passage of the right entrance region of the southwesterly jet streak.

Figure 7 reveals the profiler-derived relative vorticity values for the case study. Above 6 km, the relative vorticity values indicated anticyclonic shear vorticity when the axis of the jet was located to the northwest of the profiler triangle. During the period from 1200 UTC to 2000 UTC 29 September, the relative vorticity values indicated cyclonic shear and curvature vorticity as the axis of the jet moved through the profiler network and the axis of the 300 mb trough approached the profiler network. The relative vorticity values peaked at 2000 UTC 29 September during the passage of the 300 mb trough.

Figure 8 illustrates the profiler-derived vertical motions and the percentage of areal coverage by the precipitation echo over the profiler network. Areal coverage of the precipitation echo was derived from conventional radar data taken at the Limon, Colorado site. The coverage of the precipitation echo and the overall pattern of vertical motion are well correlated. From 1800 UTC 28 to 0400 UTC 29 September, upward motion occurred as a jet streak and a low-level trough/front passed through the network. The vertical velocities peaked at 0100 UTC 29 September in the 5 to 6 km layer. At this time, Denver's surface station was

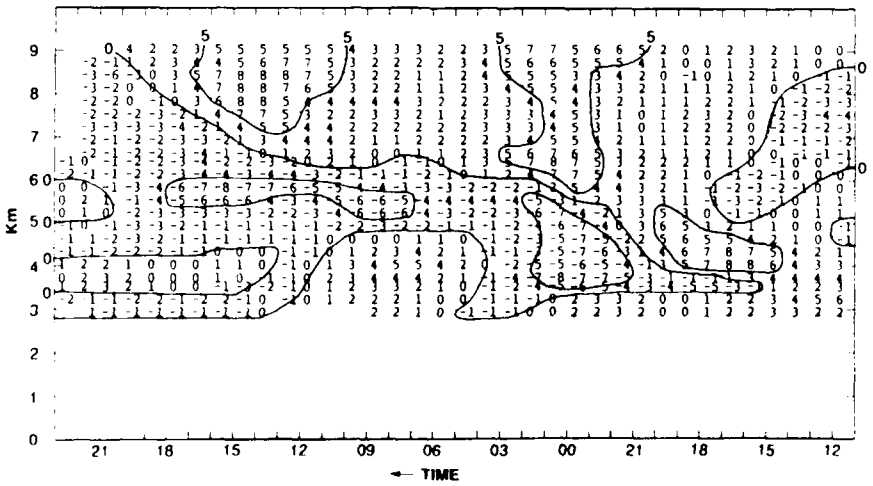

FIG. 6. Time–height section of profiler-derived horizontal divergence (units of 1×10^{-5} s^{-1}) during the period from 1200 UTC 28 to 2300 UTC 29 September 1985. Positive values denote divergence and negative values denote convergence. Contours are in 5×10^{-5} s^{-1}.

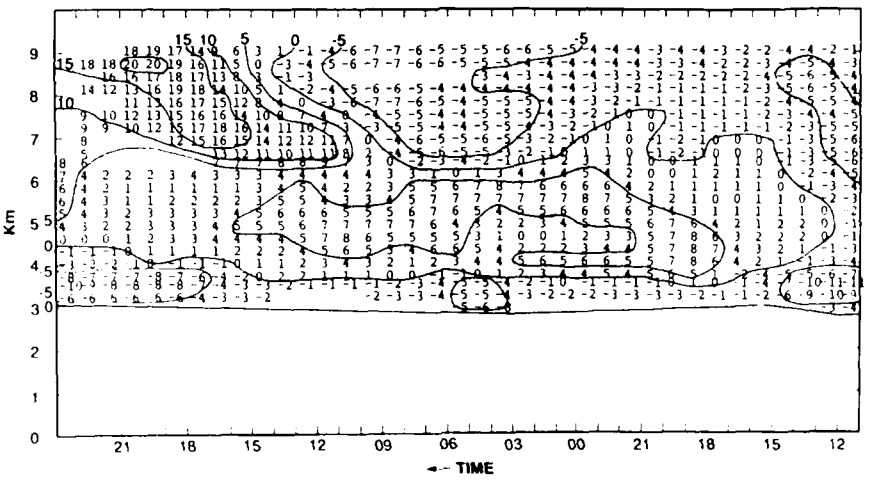

FIG. 7. As in Fig. 6 except for relative vorticity (units of 1×10^{-5} s^{-1}). Positive values represent cyclonic vorticity, and negative values represent anticyclonic vorticity. Contour interval is 5×10^{-5} s^{-1}. Blank areas denote missing data points.

reporting heavy snow with 0.4 km visibility. The secondary maxima of upward motion was associated with the passage of the 300 mb trough axis and occurred at 1800 UTC 29 September. By this time, the atmosphere had undergone strong dry advection as determined from the Denver thermodynamic sounding.

4. Conclusions

While the near-surface upslope flow provided low-level humidity and upward motions almost continually throughout the case, precipitation was heavy only when a deep layer of the troposphere became involved in the precipitation generation. Specifically, the convergence accompanying a low-level trough/front passage and the ageostrophic circulation of a southwesterly jet streak provided deep-layer upward motions during the period when the atmosphere was saturated from the surface to 400 mb. As the upper-level front entered the region, the atmosphere experienced dry advection above 700 mb, hence the termination of precipitation generation.

Comparison of the conventional synoptic-scale data

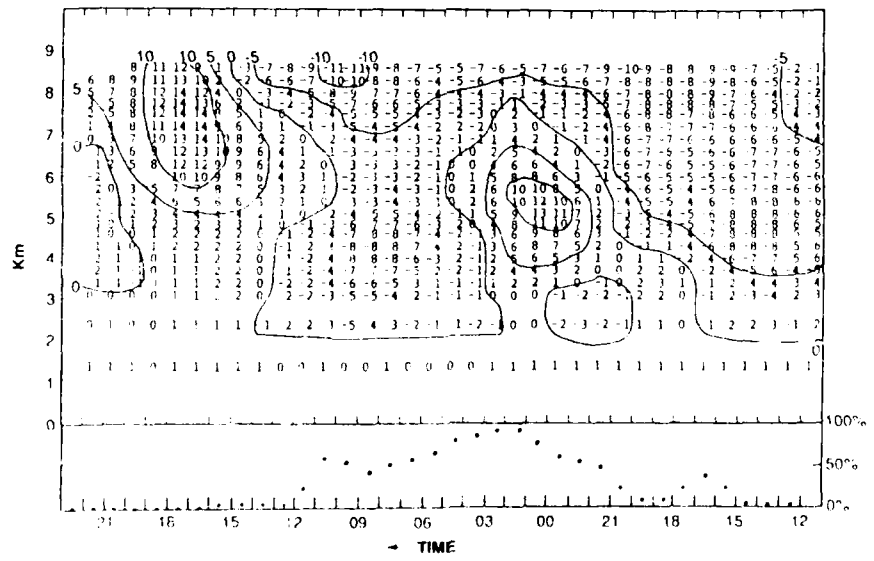

FIG. 8. Time–height section of the profiler-derived kinematic vertical velocities (cm s^{-1}) during the period from 1200 UTC 28 to 2200 UTC 29 September 1985, and a plot of percent areal coverage of the profiler triangle by the precipitation echo. Positive values denote upward motion, and negative values denote downward motion. Contour interval is 5 cm s^{-1}. Blank areas denote missing data points.

with the profiler network data reveals that the two datasets are generally consistent. Also, the profiler-derived kinematic quantities exhibit coherent vertical and temporal patterns, and these patterns change in a manner consistent with conceptual and theoretical models of the flow fields associated with upper-level short waves, jet streaks and upper-level fronts. Although the estimation of the low-level (below 3 km) vertical motions may bias the computations, the temporal variations of the profiler-derived vertical velocities are well correlated with the variations of the areal coverage of precipitation echoes over the profiler triangle during high-humidity periods. It is suggested that the profiler-derived quantities are of potential use to weather forecasters in that they enable the dynamic and kinematic interpretation of weather system structure and, thus, have nowcasting and short-term forecasting value.

Acknowledgments. The authors would like to thank Dr. Dennis W. Thomson for his advice and technical assistance during this research project, and A. S. Frisch and R. Strauch for providing the Colorado profiler network data. This research was supported by the Air Force Geophysics Laboratory under Contracts F19628-85 K-0011 and F19628-86-C-0092

REFERENCES

Augustine, J. A., and E. J. Zipser, 1987: The use of wind profilers in a mesoscale experiment. *Bull. Amer. Meteor. Soc.*, **68**, 4–17.

Balsley, B. B., 1981: The MST technique—a brief review. *J. Atmos. Terr. Phys.*, **43**, 495–509.

——, and K. S. Gage, 1982: On the use of radars for operational wind profiling. *Bull. Amer. Meteor. Soc.*, **63**, 1009–1018.

Doswell, C. A. III, and F. Caracena, 1988: Derivative estimation from marginally sampled vector point functions. *J. Atmos. Sci.*, **45**, 242–253.

Gage, K. S., and B. B. Balsley, 1978: Doppler radar probing of the clear atmosphere. *Bull. Amer. Meteor. Soc.*, **59**, 1074–1093.

Strauch, R. G., D. A. Merritt, K. P. Moran, K. B. Earnshaw and D. van de Kamp, 1984: The Colorado wind-profiling network. *J. Atmos. Oceanic Technol.*, **1**, 37–49.

Zamora, R. J., M. A. Shapiro and C. A. Doswell III, 1987: The diagnosis of upper tropospheric divergence and ageostrophic wind using profiler observations. *Mon. Wea. Rev.*, **115**, 871–884.